

# Strange Dibaryons in Neutron Stars and in Heavy-Ion Collisions

Jürgen Schaffner-Bielich<sup>a\*</sup>

<sup>a</sup>RIKEN BNL Research Center, Physics Department, Brookhaven National Laboratory, Upton, NY 11973, USA

The formation of dibaryons with strangeness are discussed for the interior of neutron stars and for central relativistic heavy-ion collisions. We derive limits for the properties of H-dibaryons from pulsar data. Signals for the formation of possible bound states with hyperons at BNL's Relativistic Heavy-Ion Collider (RHIC) are investigated by studying their weak decay patterns and production rates.

## 1. HYPERONS AND DIBARYONS IN NEUTRON STARS

There has been a lot of speculations about the appearance of new particles in the interior of neutron stars. A traditional neutron star consists of neutrons, protons, and leptons only. Cameron suggested first in 1959, that hyperons will also appear at high baryon density [1]. A possible phase transition to quark matter was conjectured shortly after the quark model was introduced [2]. Pion condensation [3] as well as kaon condensation were considered later [4]. Finally, strange stars, built out of absolutely stable strange quark matter, have been studied within the MIT bag model [5,6]. The appearance of one or the other exotic phase in the core of neutron stars is still a matter of active debates. Nevertheless, recent developments in the field indicate, that hyperons are probably the first exotic particle to appear in neutron star matter at twice normal nuclear density. This result was consistently derived within various, different models: nonrelativistic potential models [7], quark-meson coupling model [8], relativistic mean-field models [9–11], relativistic Hartree-Fock [12], Brueckner-Hartree-Fock models [13,14], and chiral effective Lagrangians [15]. Hence, the onset of hyperons at  $2\rho_0$  seems to be rather insensitive to the underlying details of the hyperon-nucleon interaction used.

If there are a lot of hyperons in the interior of neutron stars, then it might be also possible to form dibaryons with strangeness. Besides the famous H-dibaryon proposed by Jaffe [16] built out of six quarks, the most recent version of the Nijmegen potential predicts the existence of deeply bound states of two hyperons, involving the  $\Sigma$ 's and  $\Xi$ 's with maximum isospin [17]. Their results can be understood in terms of the underlying SU(3) symmetry for the baryon-baryon interactions (see [17]).

Let us assume in the following, that there exist bound states with hyperons. What would be the consequences for the properties of dense matter, as present in the interior of neutron stars? Bound systems in dense matter have been discussed before in connection

---

\*I thank RIKEN, BNL, and the U.S. Department of Energy for providing the facilities essential for the completion of this work.

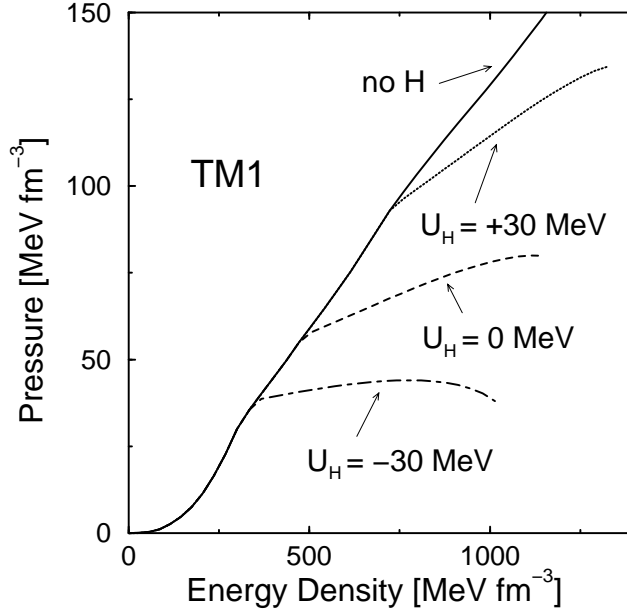


Figure 1. The equation of state of neutron star matter including a possible condensate of H-dibaryons.  $U_H$  denotes the optical potential of the H-dibaryon at normal nuclear density. For an attractive potential, the equation of state is considerably softened (taken from [18]).

with the liquid-gas phase transition of nuclear matter. They dissolve at rather low density due to effects in analogy to the Mott transition; deuterons disappear at  $1/15\rho_0$  and  $\alpha$  particles around  $1/2\rho_0$ , as detailed e.g. in [19]. A similar transition will happen for bound states with hyperons. Hence, weakly bound systems will have no influence on the equation of state of neutron star matter — unless, there is a deeply bound state which can be treated as a quasiparticle. The H-dibaryon as well as heavier quark bags with strange quarks (strangelets) are such deeply bound states. They can actually be formed as precursor of the deconfinement phase transition in the core of neutron stars. The general condition for the appearance of a strangelet in s-wave with baryon number  $A$  and charge  $Z$  is that the effective energy of the particle equals its chemical potential

$$E_s^*(k=0) = M_s + U(\rho) = A \times \mu_n - Z \times \mu_e \quad . \quad (1)$$

Here,  $U(\rho)$  stands for the effective potential felt by the strangelet at finite density. In order to estimate the effects of these exotic states, we focus on the lightest possible one, the H-dibaryon with  $A = 2$  and  $Z = 0$ . We use an extended Relativistic Mean-Field Model which incorporates the H-particle in a consistent scheme. The Lagrangian part for the H-dibaryon field reads

$$\mathcal{L}_H = D_\mu^* H^* D^\mu H - m_H^*{}^2 H^* H \quad (2)$$

with a minimal coupling scheme for the scalar and vector meson fields

$$D_\mu = \partial_\mu + ig_{\omega H} \cdot V_\mu \quad (3)$$

$$m_H^* = m_H + g_{\sigma H} \cdot \sigma \quad . \quad (4)$$

For the coupling constant to the vector field, we choose the simple quark counting rule as guidance, i.e. we set  $g_{\omega H} = 4/3g_{\omega N}$ . We fix the scalar coupling to an optical potential at normal nuclear matter density in the range

$$U_H(\rho_0) = g_{\sigma H} \cdot \sigma(\rho_0) + g_{\omega H} \cdot V_0(\rho_0) = -30 \dots + 30 \text{ MeV} \quad . \quad (5)$$

Figure 1 shows the resulting equation of state when using the parameter set TM1 and including effects from hyperons (see [18] for details). The equation of state turns out to be quite sensitive to the choice of the optical potential of the H-dibaryon. The phase transition to the H-dibaryon condensate is of second order in all cases studied. For an attractive optical potential,  $U_H(\rho_0) = -30 \text{ MeV}$ , the equation of state has a plateau-like behaviour, i.e. the pressure is very slowly rising with energy density.

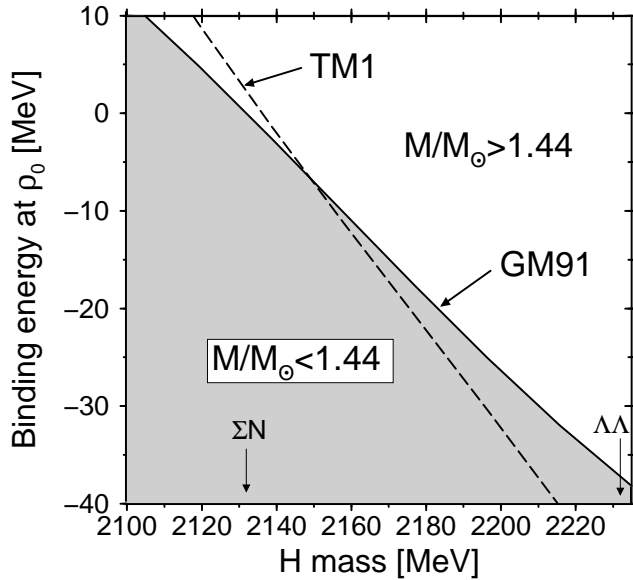


Figure 2. Neutron star constraints on the H-dibaryon from the mass of the Hulse-Taylor pulsar. A deeply bound H-dibaryon feeling an attractive potential in matter can be ruled out as the corresponding neutron stars have a too small maximum mass (from [18]).

The drastic softening of the equation of state has crucial consequences for the maximum mass of a neutron star, which will be lowered below the acceptable value of the Hulse-Taylor pulsar of  $M = 1.44M_\odot$ . Hence, one can constrain the properties of the H-dibaryon in dense matter from pulsar data. These constraints are summarized in fig. 2 as a function of the vacuum mass of the H-dibaryon and its optical potential at  $\rho_0$ . The calculations have been done by using two completely different parameterizations for the nucleon and the hyperon coupling constants (denoted as set TM1 and GM91 in the figure) and our findings seems to be rather insensitive to these choices. According to these calculations, the shaded area in the lower left side of the plot can be ruled out, as the corresponding neutron star equation of state gives too low a maximum mass. Therefore, a deeply attractive potential for the H-dibaryon with a mass close to the  $\Lambda\Lambda$  threshold is incompatible with

Table 1

The hyperon weak decay amplitudes in  $SU(3)_{\text{weak}}$  compared to experimental data. All values are in units of  $10^{-7}$ .

	parity violating		parity conserving	
	exp.	SU(3)	exp.	SU(3)
$\Lambda \rightarrow p + \pi^-$	3.25	3.25	22.1	22.1
$\Lambda \rightarrow n + \pi^-$	-2.37	-2.30	-16.0	-15.6
$\Sigma^+ \rightarrow n + \pi^+$	0.13	0.0	42.2	40.0
$\Sigma^+ \rightarrow p + \pi^0$	-3.27	-3.33	26.6	28.3
$\Sigma^- \rightarrow n + \pi^-$	4.27	4.71	-1.44	0.0
$\Xi^0 \rightarrow \Lambda + \pi^0$	3.43	3.19	-12.3	-11.7
$\Xi^- \rightarrow \Lambda + \pi^-$	-4.51	-4.51	16.6	16.6

the measured Hulse-Taylor pulsar mass. Also, a H-dibaryon mass below the  $\Sigma N$  threshold requires even a repulsive potential in matter in our model calculation to get sufficiently heavy neutron stars.

Finally, we remark that the existence of deeply bound states of two hyperons can have an indirect effect on the properties of neutron stars, though. If the hyperon-hyperon interaction is deeply attractive, it can give rise to a phase transition to hyperonic matter [20]. This phase transition can result in a drastically modified mass-radius relation for neutron stars, like neutron star twins with similar masses but smaller radii than ordinary neutron stars [21]. Hence, measurements of the mass and the radius of neutron stars will provide important insights into the equation of state and may reveal that there is indeed something strange going on at high density.

## 2. STRANGE DIBARYONS IN RELATIVISTIC HEAVY-ION COLLISIONS

There is the possibility to probe the hyperon-hyperon interaction in less remote places than neutron stars. Terrestrial relativistic heavy-ion collisions will produce dozens of hyperons in a single central collisions of two heavy nuclei, and for RHIC even close to 200 hyperons are expected [22]. The hyperons, sitting close in phase-space, can coalesce to form a bound state or a resonance which is decaying afterwards. The final products will be measured then in the detectors.

The production rates for dibaryons with hyperons at RHIC has been estimated in the coalescence model to be in the range of  $10^{-2}$  to  $10^{-4}$  per single event. Effects from the details of the dibaryon wavefunction have been found to be rather small [22]. The rapidity distribution is rather flat, so that dibaryons are also produced at forward and backward rapidities where the decay length is considerably longer than at midrapidity. The production rates can be enhanced dramatically in two ways which are not taken into account in the above coalescence estimates. If a quark-gluon plasma is formed, strange quark-antiquark pairs are produced more abundantly so that the total initial number of produced strange hadrons increases. If matter is created in a chirally restored phase, the effective hyperon masses are reduced drastically which will result in an enhanced hyperon-antihyperon yield.

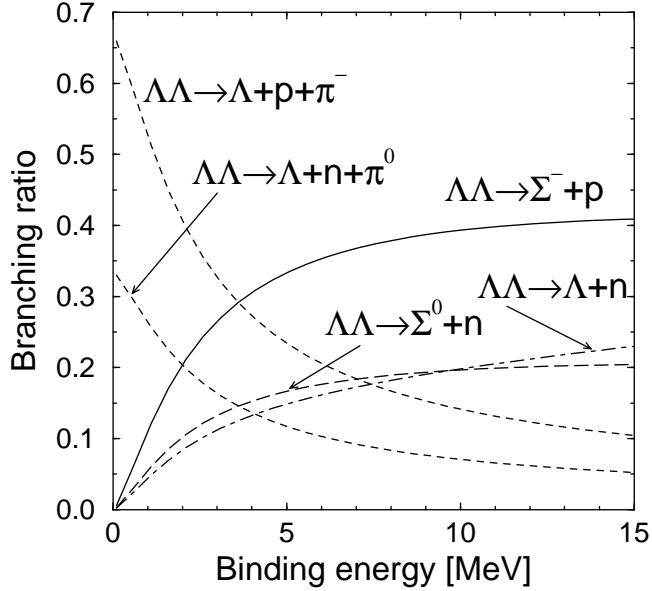


Figure 3. Branching ratios for a bound  $\Lambda\Lambda$  state as a function of its binding energy. The nonmesonic decay mode  $\Lambda\Lambda \rightarrow \Sigma^- + p$  dominates for a binding energy of 4 MeV or more (taken from [22]).

To detect strange dibaryons, their weak decay patterns have to be investigated. Starting point is the weak nonleptonic decay of hyperons in vacuum. Both, s-wave and p-wave amplitudes have been measured and correspond to a parity violating and a parity conserving amplitudes, respectively. The standard approach for describing these amplitudes is by means of chiral perturbation theory. The p-wave amplitudes are beyond leading order and are usually derived within the pole model. The basic version fails to describe the p-wave amplitudes. This constitutes the so called s-wave/p-wave puzzle for the weak nonleptonic decay of hyperons (for a discussion and more elaborate ways to remedy the situation see [23] and references therein). We have found a simple way to parameterize both amplitudes, s-wave and p-wave, in terms of pure SU(3) symmetry for the weak interactions [22]. The effective Lagrangian involves the baryon octet  $B$ , the pseudoscalar octet  $P$ , and the Gell-Mann matrix  $\lambda_6$ , which ensures the  $\Delta I = 1/2$  rule and a change of hypercharge by one unit:

$$\begin{aligned} \mathcal{L} = & D \cdot \text{Tr} \bar{B} B [P, \lambda_6] + F \cdot \text{Tr} \bar{B} [P, \lambda_6] B \\ & + G \cdot \text{Tr} \bar{B} P \gamma_5 B \lambda_6 + H \cdot \text{Tr} \bar{B} \lambda_6 \gamma_5 B P + J \cdot \text{Tr} \bar{B} \{P, \lambda_6\} \gamma_5 B \quad . \end{aligned} \quad (6)$$

The first two terms give the s-wave contributions, while the other three the p-wave contributions. Table 1 compares the resulting amplitudes with the measured ones when setting  $D = 4.72$ ,  $F = -1.62$ ,  $G = 40.0$ ,  $H = 47.8$ , and  $J = -7.1$  (in units of  $10^{-10}$ ). We conclude that the above model as defined in eq. (6) gives a reasonable description of all amplitudes.

The weak decays of possible dibaryons with hyperons are then calculated by adopting a Hulthen-type wavefunction with varying binding energy. The nonmesonic decay is described by pion- and kaon- exchange diagrams, where the weak coupling constants are

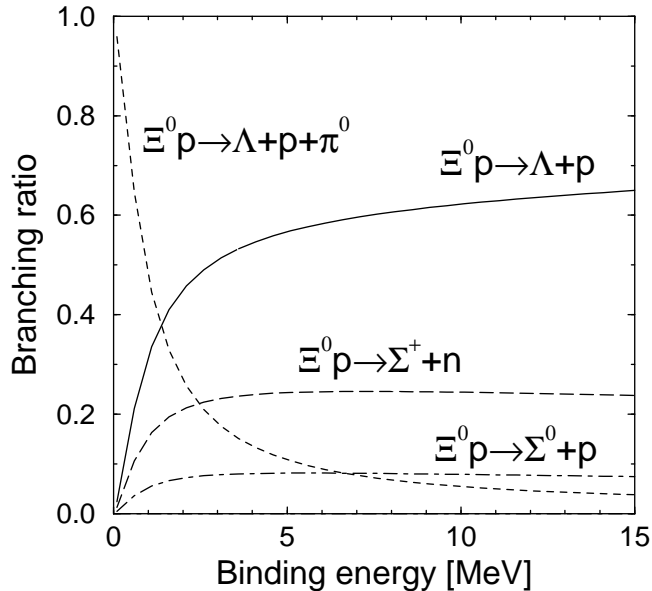


Figure 4. Branching ratios for a bound  $\Xi^0 p$  state versus its binding energy. The decay mode  $\Xi^0 p \rightarrow \Lambda p$  has the largest branching ratio for binding energies of 1.5 MeV or more (from [22]).

given by eq. (6) and the strong coupling constants by SU(6) symmetry. We note in passing, that the state-of-the-art calculations for the weak nonmesonic decay of hypernuclei rely on the (wrong) pole model (see [24] and references therein). While this will not affect the pion exchange diagrams, accidentally, it will certainly alter the coupling constants for the kaon exchange diagrams. The use of the SU(3) symmetric model might be interesting to pursue in this direction to investigate possible effects, e.g. for the ratio of neutron- to proton-induced decay which comes out too small in the standard approach.

Figure 3 depicts the branching ratio for a bound  $\Lambda\Lambda$  system versus the binding energy, and fig. 4 shows the case for a possible  $\Xi^0 p$  dibaryon. The mesonic decay channel dominates for binding energies of a few MeV. Then, for higher binding energies, the nonmesonic decay channels take over. For  $\Lambda\Lambda$ , the dominant nonmesonic decay mode is to a  $\Sigma^-$  and a proton, the same as for the hypothetical H-particle. The  $\Xi^0 p$  decays mainly to a  $\Lambda$  and a proton for binding energies of just 1.5 MeV and more. This weak decay has the same decay topology as the weak decay of the  $\Xi^-$  and the  $\Omega^-$ , and both particles have readily been measured in relativistic heavy-ion collisions [25]. Other interesting decay topologies occur for the doubly negatively charged dibaryons  $\Sigma^-\Sigma^-$ ,  $\Sigma^-\Xi^-$ , and  $\Xi^-\Xi^-$ , all of which have been predicted to be bound in the recent Nijmegen model [17]. Here, a negatively charged object decays into two negatively charged tracks — a unique decay prong which should be easily seen in tracking devices. The calculated lifetimes of all dibaryons are lying just below the one for the free  $\Lambda$  with decay lengths in the range of  $c\tau = 1\text{--}5$  cm.

There are in principle three ways to detect possible short-lived strange dibaryons (for an experimental investigation we refer to the detailed feasibility study of Coffin and Kuhn for the case of the H-dibaryon at the STAR detector [26]). Firstly, if the dibaryon is bound, one can look for exotic decays in a TPC, like a charged track splitting into two charged

ones. Secondly, if the mass of the strange dibaryon is close to threshold, it will show up in the invariant mass spectrum of its decay products by using background subtraction. Note, that this method is also sensitive to dibaryon resonances, if their decay widths are not too large [27]. Thirdly, the hyperon-hyperon interaction and possible broad dibaryon resonances can be probed in correlation functions as the low momentum part is sensitive to final state interactions [28,29].

## REFERENCES

1. A. G. W. Cameron, *Astrophys. J.* 130 (1959) 884.
2. D. D. Ivanenko, D. F. Kurdgelaidze, *Astrophys. J.* 1 (1965) 251.
3. A. B. Migdal, *Rev. Mod. Phys.* 50 (1978) 107.
4. D. B. Kaplan, A. E. Nelson, *Phys. Lett. B* 175 (1986) 57, erratum: *ibid* 179 (1986) 409.
5. P. Haensel, J. L. Zdunik, R. Schaeffer, *Astron. Astrophys.* 160 (1986) 121.
6. C. Alcock, E. Farhi, A. Olinto, *Astrophys. J.* 310 (1986) 261.
7. S. Balberg, A. Gal, *Nucl. Phys. A*625 (1997) 435.
8. S. Pal, M. Hanauske, I. Zakout, H. Stöcker, W. Greiner, *Phys. Rev. C* 60 (1999) 015802.
9. N. K. Glendenning, *Astrophys. J.* 293 (1985) 470.
10. R. Knorren, M. Prakash, P. J. Ellis, *Phys. Rev. C* 52 (1995) 3470.
11. J. Schaffner, I. N. Mishustin, *Phys. Rev. C* 53 (1996) 1416.
12. H. Huber, F. Weber, M. K. Weigel, C. Schaab, *Int. J. Mod. Phys. E*7 (1998) 301.
13. M. Baldo, G. F. Burgio, H. J. Schulze, *Phys. Rev. C* 61 (2000) 055801.
14. I. Vidana, A. Polls, A. Ramos, L. Engvik, M. Hjorth-Jensen, *Phys. Rev. C* 62 (2000) 035801.
15. M. Hanauske, D. Zschesche, S. Pal, S. Schramm, H. Stöcker, W. Greiner, *Astrophys. J.* 537 (2000) 50320.
16. R. L. Jaffe, *Phys. Rev. Lett.* 38 (1977) 195, erratum: *ibid* 38 (1977) 617.
17. V. G. J. Stoks, T. A. Rijken, *Phys. Rev. C* 59 (1999) 3009.
18. N. K. Glendenning, J. Schaffner-Bielich, *Phys. Rev. C* 58 (1998) 1298.
19. G. Röpke, L. Münchow, H. Schulz, *Nucl. Phys. A*379 (1982) 536.
20. J. Schaffner-Bielich, A. Gal, *Phys. Rev. C* 62 (2000) 034311.
21. J. Schaffner-Bielich, M. Hanauske, H. Stöcker, W. Greiner, [astro-ph/0005490](https://arxiv.org/abs/hep-ph/0005490) .
22. J. Schaffner-Bielich, R. Mattiello, H. Sorge, *Phys. Rev. Lett.* 84 (2000) 4305.
23. B. R. Holstein, [hep-ph/0010125](https://arxiv.org/abs/hep-ph/0010125) .
24. A. Parreno, A. Ramos, C. Bennhold, *Phys. Rev. C* 56 (1997) 339.
25. E. Quercigh, contribution to these proceedings.
26. J. P. Coffin, C. Kuhn, *J. Phys. G* 23 (1997) 2117.
27. S. D. Paganis, G. W. Hoffmann, R. L. Ray, J. L. Tang, T. Udagawa, R. S. Longacre, *Phys. Rev. C* 62 (2000) 024906.
28. F. Wang, S. Pratt, *Phys. Rev. Lett.* 83 (1999) 3138.
29. A. Ohnishi, Y. Hirata, Y. Nara, S. Shinmura, Y. Akaishi, *Nucl. Phys. A*670 (2000) 297.